

EXHIBIT 3

The Influence of Antisense Oligonucleotide Length on Dystrophin Exon Skipping

PL Harding¹, AM Fall¹, K Honeyman¹, S Fletcher¹ and SD Wilton¹

¹Experimental Molecular Medicine Group, Centre for Neuromuscular and Neurological Disorders, University of Western Australia, Nedlands, Perth, Western Australia, Australia

Antisense oligonucleotides (AOs) can be used to redirect dystrophin pre-messenger RNA (mRNA) processing, to remove selected exons from the mature dystrophin mRNA, to overcome nonsense mutations, and/or restore the reading frame. Redundancy within the dystrophin protein allows some domains to be removed without seriously compromising function. One of the challenges for splicing blockade is to design AOs that efficiently remove targeted exons across the dystrophin pre-mRNA. AOs are initially designed to anneal to the more obvious motifs implicated in the splicing process, such as acceptor or donor splice sites and *in silico* predicted exonic splicing enhancers. The AOs are evaluated for their ability to induce targeted exon skipping after transfection into cultured myoblasts. Although no single motif has been implicated in the consistent induction of exon skipping, the length of the AO has emerged as an important parameter in designing compounds that redirect dystrophin pre-mRNA processing. We present data from *in vitro* studies in murine and human cells showing that appropriately designed AOs of 25–31 nucleotides are generally more effective at inducing exon skipping than shorter counterparts. However, there appears to be an upper limit in optimal length, which may have to be established on a case-by-case basis.

Received 26 March 2006; accepted 24 August 2006.
doi:10.1038/sj.mt.6300006

INTRODUCTION

Duchenne muscular dystrophy (DMD) is a severe and debilitating disorder arising from mutations within the dystrophin gene that preclude synthesis of functional dystrophin protein.¹ Dystrophin is a crucial structural protein that anchors cytoskeletal actin to the sarcolemmal membrane in skeletal and smooth muscle cells.² In the absence of functional dystrophin, normal muscle contractions cause injury to the sarcolemmal membrane. In response to repeated membrane damage, the regenerative capacity of the muscle is overwhelmed, and the

tissue is replaced by adipose and fibrous material (for a review see refs. 3,4).

The human dystrophin gene is the largest known and has 79 exons spanning 2.4 million bases.⁵ The most common type of dystrophin mutation is a genomic deletion of one or more exons, occurring predominately in two hotspots involving the 5' end and exons 44–55.⁶ However, approximately one-third of mutations are more subtle DNA changes (nonsense mutations, splicing defects, micro-deletions/insertions) and these appear to be spread across the entire dystrophin gene (for a review see ref. 4).

Becker muscular dystrophy also arises from dystrophin gene defects, but these are typically in-frame deletions that still allow production of shorter but partially functional dystrophin protein.⁷ Depending upon the position and size of these in-frame deletions, clinical progression can be delayed and associated with mild to barely detectable symptoms.⁸ For example, one Becker muscular dystrophy patient had such mild symptoms that he was not diagnosed with an exon 3–9 deletion until the age of 65 years.⁹ Another patient with a 12 exon deletion (exons 33–44) only experienced mild muscular cramping after intensive exercise.¹⁰

Antisense oligonucleotides (AOs) have been used to mask abnormal or cryptic splice sites and restore normal pre-messenger RNA (mRNA) processing.¹¹ AOs may be applied to a dystrophin gene transcript, carrying a protein-truncating mutation, to target normal splice motifs and induce abnormal splicing to remove the exon carrying the nonsense mutation or restore the reading frame around a deletion.¹² Many aspects of the dystrophin gene, such as size, and the complexity of processing and expression, which have proved to be great challenges for gene repair or replacement,¹³ may be regarded as positive features with respect to AO-induced exon skipping.

The *mdx* mouse model of muscular dystrophy¹⁴ arises from a nonsense mutation in dystrophin exon 23 that precludes the synthesis of a full-length dystrophin protein.¹⁵ Although this animal model does not reflect the clinical severity of DMD, the *mdx* mouse has been useful in studying dystrophin at the molecular level. Initial attempts to overcome this *mdx* mutation by AO-induced exon skipping used a 12mer of 2'-O-methyl bases on a phosphorothioate backbone targeting the acceptor site of

Correspondence: SD Wilton, Experimental Molecular Medicine Group, Centre for Neuromuscular and Neurological Disorders, University of Western Australia, 4th Floor, A block, QE 11 Medical Centre, Verdun Street, Nedlands, Perth 6009, Western Australia, Australia. E-mail: swilton@cyllene.uwa.edu.au

intron 22, but precise removal of exon 23 was not demonstrated *in vitro*.¹⁶ Wilton *et al.*¹² designed a 20mer, designated M23D(+12–08), directed at the *mdx* mouse exon 23 donor splice site, which induced consistent exon 23 skipping in a dose-dependent manner. The first refinement to AO design was made with M23D(+12–13), which targeted the same coordinates with additional intronic sequence.¹⁷ A subsequent improvement was then achieved with a 20mer that annealed to the last two bases of exon 23 and the first 18 bases of intron 23, M23D(+02–18).¹⁷ Here, we report further enhancement of exon skipping with M23D(+07–18) directed at the same donor splice site, and show that AO length can play a crucial role in determining efficiency of targeted exon removal. We have found this trend extends to other splice sites in the human dystrophin gene transcript and report enhanced exon skipping of human dystrophin exons 16, 51, and 53 with optimized AOs.

RESULTS

For a full explanation of AO nomenclature, please refer to the **Table 1** legend.

Murine studies

Four AOs, a 20mer M23D(+02–18), the 25mer M23D(+07–18), and two 30mers M23D(+12–18) and M23D(+07–23) (**Table 1**), were compared for their ability to induce exon 23 skipping in the *mdx* dystrophin mRNA. As shown in **Figure 1**, both the 20 and 25mers induced exon skipping at 10 nM concentration; however, the 25mer was consistently able to induce more pronounced exon skipping at day 1 (**Figure 1a** and **b**). After transfection at 100 and 200 nM, the 25mer induced approximately 74 and 82% exon skipping, respectively, whereas the 20mer induced 32 and 68% exon skipping at equivalent concentrations, based upon densitometry using a Chemi-Smart 3,000 gel documentation system and Bio-1D analysis software (Vilber Lourmat, Marne La Vallée).

The 20 and 25mers were then compared for their ability to induce sustained exon skipping at 3, 5, and 7 days after transfection. Three days after transfection, the 20mer only induced weak exon skipping at 25 nM whereas M23D(+07–18) was still able to induce exon skipping at 10 nM concentration (**Figure 1c** and **d**). Although exon skipping in cells treated with the 20mer was barely detectable at day 5, the 25mer induced moderate levels of exon skipping at 200 nM with some exon skipping still observed 5 days after transfection at 50 nM (**Figure 1e** and **f**). No detectable exon skipping was induced by the 20mer, and only low levels of exon skipping were observed after transfection with the 25mer at 100 nM at day 7 (data not shown).

In contrast to the high levels of exon skipping induced by the 20mer and 25mer, the two 30mers had little effect on exon 23 exclusion from the mature dystrophin mRNA. The two 30mers, which span the same site as the most effective AO, M23D(+07–18), but extend annealing by five nucleotides in the 5' or 3' directions, were unable to induce efficient exon 23 exclusion (**Figure 1g** and **h**). Note that M23D(+07–23) appeared marginally more effective at exon 23 excision than the other 30mer M23D(+12–18).

Human studies

A panel of AOs was directed at acceptor, donor, and exonic splicing enhance (ESE) sites within human dystrophin exon 16 (**Table 1**). Serine-arginine (SR)-rich proteins are involved in exon selection during splicing and predicted SR protein binding sites for exon 16 are shown in **Figure 2a**. The locations of AOs directed at and near the acceptor site are shown in the expanded detail. AOs targeting the donor site were ineffective (data not shown), whereas masking an intra-exonic domain predicted to contain ESEs with H16A(+87+109) induced only moderate exon 16 skipping (data not shown). However, annealing a 25mer, H16A(–06+19) targeted to the acceptor site and adjacent putative ESEs, induced enhanced exon 16 removal (**Figure 2b**) compared to that induced by H16A(+87+109). A series of AOs were subsequently designed to this region to further refine and optimize induced exon skipping. The majority of AOs directed at or near the exon 16 acceptor site were found to induce consistent exon skipping, generally in a dose-dependent manner; however, there was considerable variation in efficiency of exon 16 removal (**Figure 2b–g**). The two 31mers induced strong exon skipping at 10 nM (**Figure 2e** and **f**) and the only AO that failed to induce exon 16 skipping was a 20mer, H16A(–07+13) (**Figure 2g**), despite this compound annealing to sequences common to both the 31mers that efficiently dislodged exon 16 from the mature mRNA.

Table 2 summarizes the exon skipping potential of each AO observed after *in vitro* transfection, and also indicates weighted matrix values of predicted SR motifs that are masked by AOs designed to the target exons. It should be noted that an AO may mask more than one SR motif.

Exon 51 skipping could be induced at low levels by several AOs directed at various intra-exonic targets (**Table 2**). However, enhanced exon skipping was identified after targeting one region with H51A(+66+90) and H51A(+66+95), but in this particular example, there was only a minor improvement in induced exon skipping when using the longer AO (**Figure 3**). Data from two separate experiments are shown in **Figure 3a** and **b** to demonstrate reproducibility of exon skipping *in vitro*.

AO-induced exon 53 removal also showed similar trends to exon 51 in that many of the AOs induced low levels of exon skipping, but only when applied at high concentrations of 200 nM or above. Putative SR-binding domains and the arrangement of some of the amenable targets is indicated in **Figure 4a**. H53A(+39+62) induced a low level of exon 53 skipping (**Figure 4b**), and this region was selected for subsequent AO refinement. A 25mer, H53A(+45+69) was also found to induce very weak exon skipping at 600 nM (**Figure 4c**), whereas a 31mer, H53A(+39+69), spanning the entire region covered by these 25mers was found to induce exon skipping after transfection at 10 nM (**Figure 4d**).

DISCUSSION

The concept of exon skipping to address DMD mutations is gaining considerable attention as a potential therapy for this devastating condition. Significant progress in this field is leading to clinical trials to demonstrate safety and proof of principle.¹⁸

Table 1 Sequences of 2'-O-methyl AOs used in this study

| Nomenclature | Sequence (5'-3') | Size (bp) | % G:C content |
|----------------|---|-----------|---------------|
| H16A(-17+08) | UUU AAA ACC UGU UAA AAC AAG AAA G | 25 | 24 |
| H16A(-12+19) | CUA GAU CCG CUU UUA AAA CCU GUU AAA ACA A | 31 | 32 |
| H16A(-06+19) | CUA GAU CCG CUU UUA AAA CCU GUU A | 25 | 36 |
| H16A(-06+25) | UCU UUU CUA GAU CCG CUU UUA AAA CCU GUU A | 31 | 32 |
| H16A(-07+13) | CCG CUU UUA AAA CCU GUU AA | 20 | 35 |
| H16A(+01+25) | UCU UUU CUA GAU CCG CUU UUA AAA C | 25 | 32 |
| H16A(+06+30) | CUU UUU CUU UUC UAG AUC CGC UUU U | 25 | 32 |
| H16A(+11+35) | GAU UGC UUU UUC UUU UCU AGA UCC G | 25 | 36 |
| H16A(+12+37) | UGG AUU GCU UUU UCU UUU CUA GAU CC | 26 | 36 |
| H16A(+45+67) | GAU CUU GUU UGA GUG AAU ACA GU | 23 | 35 |
| H16A(+87+109) | CCG UCU UCU GGG UCA CUG ACU UA | 23 | 52 |
| H16A(+92+116) | CAU GCU UCC GUC UUC UGG GUC ACU G | 25 | 56 |
| H16A(+105+126) | GUU AUC CAG CCA UGC UUC CGU C | 22 | 54 |
| H16D(+11-11) | GUA UCA CUA ACC UGU GCU GUA C | 22 | 45 |
| H16D(+05-20) | UGA UAA UUG GUA UCA CUA ACC UGU G | 25 | 36 |
| H51A(-01+25) | ACC AGA GUA ACA GUC UGA GUA GGA GC | 26 | 50 |
| H51A(+61+90) | ACA UCA AGG AAG AUG GCA UUU CUA GUU UGG | 30 | 40 |
| H51A(+66+90) | ACA UCA AGG AAG AUG GCA UUU CUA G | 25 | 43 |
| H51A(+66+95) | CUC CAA CAU CAA GGA AGA UGG CAU UUC UAG | 30 | 40 |
| H51A(+111+134) | UUC UGU CCA AGC CCG GUU GAA AUC | 24 | 50 |
| H51A(+175+195) | CAC CCA CCA UCA CCC UCU GUG | 21 | 62 |
| H51A(+199+220) | AUC AUC UCG UUG AUA UCC UCA A | 22 | 36 |
| H51D(+08-17) | AUC AUU UUU UCU CAU ACC UUC UGC U | 25 | 32 |
| H51D(+16-07) | CUC AUA CCU UCU GCU UGA UGA UC | 23 | 43 |
| H53A(-07+18) | GAU UCU GAA UUC UUU CAA CUA GAA U | 25 | 28 |
| H53A(-12+10) | AUU CUU UCA ACU AGA AUA AAA G | 22 | 23 |
| H53A(+23+47) | CTG AAG GTG TTC TTG TAC TTC ATC C | 25 | 44 |
| H53A(+39+62) | CUG UUG CCU CCG GUU CUG AAG GUG | 24 | 58 |
| H53A(+39+69) | CAU UCA ACU GUU GCC UCC GGU UCU GAA GGU G | 31 | 52 |
| H53A(+45+69) | CAU UCA ACU GUU GCC UCC GGU UCU G | 25 | 52 |
| H53A(+124+145) | UUG GCU CUG GCC UGU CCU AAG A | 22 | 55 |
| H53A(+151+175) | GUA UAG GGA CCC UCC UUC CAU GAC U | 25 | 52 |
| H53D(+09-18) | GGU AUC UUU GAU ACU AAC CUU GGU UUC | 27 | 37 |
| H53D(+14-07) | UAC UAA CCU UGG UUU CUG UGA | 21 | 38 |
| M23D(+07-18) | GGC CAA ACC UCG GCU UAC CUG AAA U | 25 | 52 |
| M23D(+02-18) | GGC CAA ACC UCG GCU UAC CU | 20 | 60 |
| M23D(+12-18) | GGC CAA ACC UCG GCU UAC CUG AAA UUU UCG | 30 | 50 |
| M23D(+07-23) | UUA AAG GCC AAA CCU CGG CUU ACC UGA AAU | 30 | 43 |

AO, antisense oligonucleotide. AO nomenclature is based upon target species (H, human, M, mouse), exon number, and annealing coordinates as described by Mann *et al.*²⁷ The number of exonic nucleotides from the acceptor site is indicated as a positive number, whereas intronic bases are given a negative value. For example, H16A(-06+25) refers to an AO for human dystrophin exon 16 acceptor region, at coordinates 6 intronic bases from the splice site to 25 exonic bases into exon 16. The total length of this AO is 31 nucleotides and it covers the exon 16 acceptor site.

Exon 51 has been chosen for the “first time in human” studies, as removing this exon could restore the reading frame in a substantial number of DMD patients who have deletions in the major mutation hotspot of the dystrophin gene.¹⁹ These trials

will rely on direct intramuscular injections to deliver the AOs into dystrophic muscle, in sufficient amounts to restore dystrophin expression in a localized area. If no adverse events are reported, and molecular testing confirms exon 51 exclusion

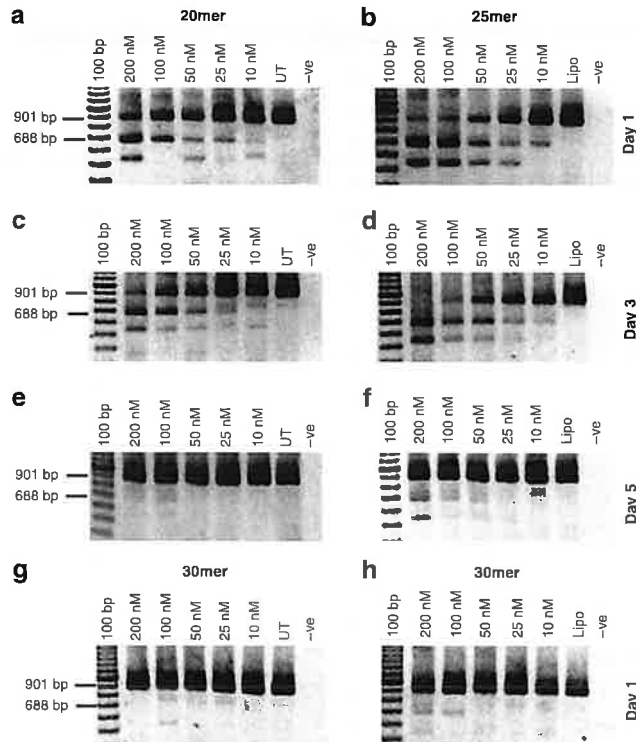


Figure 1 RT-PCR analysis showing exon skipping induced by AOs directed at mouse dystrophin exon 23. The intact dystrophin transcript is represented by a 901 bp product, and the shorter product (688 bp) corresponds to transcripts excluding exon 23. A 542 bp product that corresponding to skipping of both exons 22 + 23 is evident in some lanes and has been reported previously.¹⁷ (**a**, **c**, and **e**) Levels of exon skipping induced by the 20mer, M23D(+02–18) at days 1, 3, and 5 post-transfection. (**b**, **d**, and **f**) Exon skipping induced by the 25mer AO, M23D(+07–18) at days 1, 3, and 5 post-transfection. (**g** and **h**) Levels of exon skipping induced by the 30mers M23D(+12–18) and M23D(+07–23), respectively, 24 h post-transfection. Untreated controls are indicated as UT, transfection reagent controls are indicated as Lipo (Lipofectin), and PCR-negative controls are indicated –ve.

and dystrophin production, subsequent trials will be initiated to evaluate exon skipping, using systemic AO delivery. Additional trials will be required to address other targets within the dystrophin gene transcript, as one limitation of AO-induced exon skipping is that this therapy must be customized for each distinct dystrophin mutation. Consequently, a panel of AOs are required to address mutations across the dystrophin gene, and it is essential that the most effective compounds are taken to the clinic.

We classify an effective AO as one that induces strong, consistent, and sustained exon skipping, preferably after administration at concentrations in the range of 10–50 nM, as assayed in myogenic cells *in vitro*. This classification is somewhat arbitrary in that many of the AOs developed in our laboratory can induce substantial levels of exon skipping, but only after administration at concentrations of 200 nM or higher. The more efficacious AOs can induce sustained and pronounced exon skipping when applied at lower concentrations. The 20 and 25mers, M23D(+02–18) and M23D(+07–18), induced similar levels

of murine dystrophin exon 23 skipping after *in vitro* transfection at concentrations of 200 nM or higher. However, the longer AO must be regarded as the preferred compound as it is effective at lower concentrations and shows extended duration of induced exon skipping. It would also be preferable to use AOs at the lowest possible concentration to minimize the cost of treatment, extend the therapeutic action of exon skipping, and also reduce the risk of non-specific effects, which is of particular relevance with certain AO chemistries (for a review see refs. 20,21).

We have used normal human myogenic cells to aid in the design of AOs that target dystrophin exons, as this system allows all of the dystrophin exons to be examined using the natural human splicing machinery. The humanized DMD mouse²² has been proposed as a model in which to design and evaluate AOs for the treatment of DMD. We urge caution in manipulating human dystrophin gene expression on a background of mouse splicing machinery. In addition, modifying normal dystrophin expression also sets a higher “bench mark” for inducing and maintaining out-of-frame transcripts. Removal of certain exons from the normal dystrophin transcript will mimic DMD-associated gene deletions, disrupt the reading frame, and render the induced transcripts susceptible to rapid turnover through nonsense-mediated decay. In some dystrophic muscle, the levels of dystrophin mRNA are reportedly a fraction of those in normal muscle.²³ If only low levels of exon skipping could be induced in dystrophic cells, there may be insufficient mRNA to produce therapeutic levels of dystrophin. We would anticipate that appropriately induced exon skipping should by-pass protein-truncating mutations, restore the reading frame, and rescue the transcript from nonsense-mediated decay. We would then expect in-frame dystrophin transcripts to accumulate, thus increasing dystrophin expression, although this has yet to be confirmed.

We have found that designing an AO to induce efficient exon skipping can be a unique challenge for each individual exon. In some cases, exon removal was easily and efficiently induced by targeting a variety of motifs. Previously, we and others showed that exon 19 skipping could be induced at high levels by targeting either acceptor, donor, or ESE sites with AOs that varied in length from 12 to 31 nucleotides.^{24–26} A 31mer was the most efficient at inducing exon 19 skipping and shorter AOs that annealed within the 31mer coordinates showed reduced capacity to dislodge this exon from the mRNA, a trend most pronounced at lower transfection concentrations.²⁴ This provided one of the first examples showing that longer AOs tend to be more effective at inducing targeted exon skipping.

We have previously demonstrated that refinement in AO design directed at the donor splice site of murine dystrophin exon 23 could result in enhanced exon skipping.^{12,17,27,28} The M23D(+02–18) had been regarded as our optimal compound, until this report in which we directly compared M23D(+02–18) with the longer M23D(+07–18), and found the latter induced enhanced exon 23 skipping. Further increases in AO length, prompted by studies addressing some human dystrophin targets, were found to be counter-productive with respect to mouse dystrophin exon 23 skipping. The longer AOs, M23D(+12–18) and M23D(+07–23), were much less

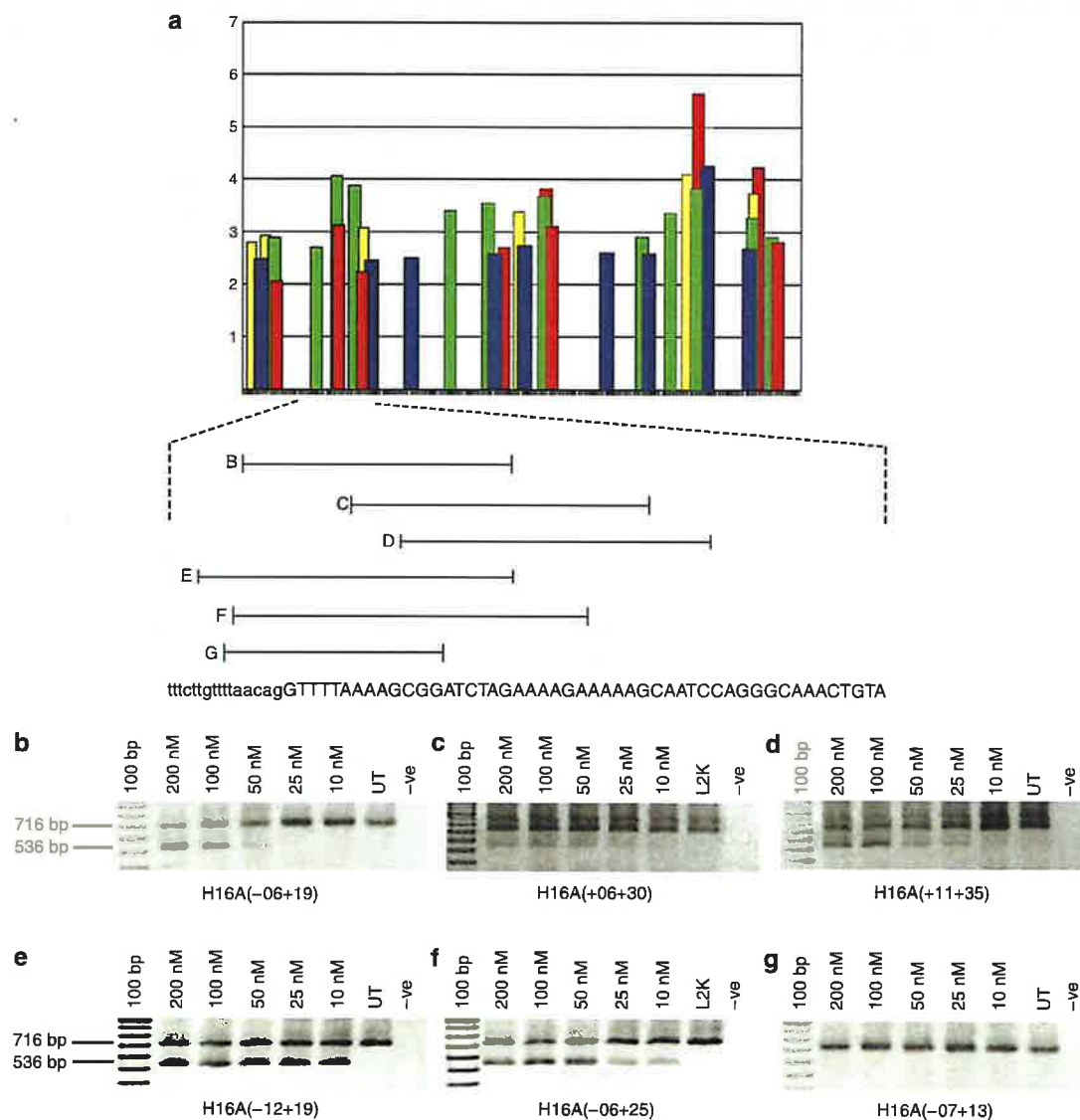


Figure 2 Induction of exon 16 skipping in the human dystrophin gene transcript. **(a)** Putative SR-binding sites for human dystrophin exon 16, as predicted by ESEfinder 2.0, SF2/ASF (red), SC35 (blue), SRp40 (green), and SRp55 (yellow).³⁰ The nucleotide sequence analyzed by ESEfinder included exons 16 and 50 flanking intronic bases (X axis). The acceptor splice site and flanking sequence targeted by the AOs is expanded. **(b-g)** RT-PCR of exon skipping induced by AOs as specified, 24 h after transfection. The intact transcript is represented by a product of 716 bp, whereas the transcript product missing exon 16 is 536 bp. Untreated controls are indicated as UT, transfection reagent controls are indicated as L2K (Lipofectamine 2000), and PCR-negative controls are indicated -ve.

effective at removing exon 23 from the mature dystrophin mRNA, and this may reflect influences of secondary structure of the dystrophin mRNA in that area.

The program Mfold²⁹ was used to analyze potential secondary structures occurring in the AOs, as these 2'-O-methyl compounds are regarded as RNA-like. *In silico* analysis of AO folding indicated the same potential self-annealing (three G:Cs and one G:U) in the two AOs that induced strong mouse dystrophin exon 23 skipping, M23D(+02-18) and M23D(+07-18), and one of the 30mers, M23D(+12-18). The other 30mer, M23D(+07-23) that induced slightly better exon 23 skipping than M23D(+12-18), contained one

additional A:U pair in the four nucleotide duplex (data not shown); hence, we consider AO secondary structure an unlikely factor contributing to the inability of the 30mers to induce exon skipping.

Human dystrophin exons 16, 51, and 53 are examples in which induction of efficient exon skipping was not readily achieved. We found no definitive method to predict amenable sites within the pre-mRNA that, when targeted with an AO, would ensure efficient exon excision. For example, ESEfinder³⁰ predicted a cluster of strong SR-binding sites (based on threshold score for each of the four SR proteins) near the 3' end of exon 16, adjacent to the donor splice site. ESEfinder includes a caveat

Table 2 A summary of AO efficiency with respect to targeted exon skipping and predicted SR-binding sites—ESEfinder 2.0³⁰

| Nomenclature | Skipping efficiency | SF2/ASF | SC35 | SRp40 | SRp55 |
|-----------------|---------------------|-----------|-----------|----------------|-------|
| H16A(−17 +08) | + | 3.12 | — | 4.05/3.87/2.69 | — |
| H16A(−12+19) | ++ | 3.13/2.24 | 2.46 | 4.06/3.87 | 3.07 |
| H16A(−06+19) | + | 3.13/2.24 | 2.46 | 4.06/3.87 | 3.07 |
| H16A(−06+25) | ++ | 3.13/2.24 | 2.46 | 4.06/3.87 | 3.07 |
| H16A(−07+13) | — | 3.13 | — | 4.06/3.87 | 3.07 |
| H16A(+01+25) | — | 2.24 | 2.45 | 3.87 | 3.06 |
| H16A(+06+30) | + | 2.24 | 2.45 | — | — |
| H16A(+11+35) | + | — | 2.45 | — | 3.06 |
| H16A(+12+37) | — | — | 2.45/2.49 | — | — |
| H16A(+45+67) | — | — | — | 3.39 | — |
| H16A(+87+109) | + | 3.82/3.11 | 2.74 | 3.67 | 3.39 |
| H16A(+92+116) | — | 3.82/3.11 | — | 3.67 | — |
| H16A(+105 +126) | — | — | — | — | — |
| H16D(+11−11) | — | 5.63 | 4.26 | 3.82 | 4.10 |
| H16D(+05−20) | — | 5.63 | 4.26 | 3.82 | — |
| H51A(−01+25) | + | 3.49/2.05 | 2.78 | 2.72/3.08/3.98 | — |
| H51A(+61+90) | ++ | 2.16 | — | — | — |
| H51A(+66+90) | ++ | — | — | — | — |
| H51A(+66+95) | ++ | — | — | — | — |
| H51A(+111+134) | — | 2.56 | 3.05/2.58 | 3.55/2.71 | — |
| H51A(+175+195) | — | 5.01/2.68 | — | 3.94/3.55 | 2.91 |
| H51A(+199+220) | — | 2.24 | — | 2.88 | 2.81 |
| H51D(+08−17) | — | 3.09 | — | — | — |
| H51D(+16−07) | + | 3.09 | — | — | — |
| H53A(−7+18) | — | — | 3.07 | 3.10 | — |
| H53A(−12+10) | — | — | 3.07 | 3.10 | — |
| H53A(+23+47) | +/− | — | — | 3.19/2.94 | — |
| H53A(+39+62) | +/− | 3.08/2.48 | — | 3.19 | — |
| H53A(+39+69) | ++ | 3.08/2.48 | — | 3.19 | — |
| H53A(+45+69) | + | 3.08 | — | 3.19 | — |
| H53A(+124+145) | — | 2.55/2.2 | 4.04 | 3.4/3.0/2.89 | — |
| H53A(+151+175) | +/− | 2.06 | 5.43 | — | — |
| H53D(+09−18) | +/− | — | 3.81 | — | — |
| H53D(+14−07) | +/− | 3.40 | 3.81 | 3.90 | 2.90 |

AO, antisense oligonucleotide. The threshold scores predicted here by ESEfinder are shown for each AO and additionally, correspond to peaks illustrated in **Figure 2a** for exon 16, and **Figure 4a** for exon 53.

stating “the presence of a high score motif does not necessarily identify that sequence as an ESE in its native context. For example, a nearby silencer element may prevent the SR protein from binding”. Nevertheless, this *in silico* prediction provided a useful starting point and suggested the exon 16 donor region was an appropriate target for AOs to influence splicing and promote exon exclusion. Masking these domains, in addition to the donor splice site, with several different AOs failed to induce any detectable exon 16 skipping. However, directing AOs at the beginning of this exon induced strong and sustained exon skipping, but only after transfection with AOs of adequate

length. Two 31mers, three 25mers, and a 20mer annealed to the similar overlapping coordinates within human dystrophin exon 16 and all, except the shortest AO H16A(−07 + 13), induced some exon 16 skipping. Exon 16 removal was never observed after transfection with the 20mer, H16A(−07 + 13). Although there was no evidence of any AO synthesis problems with this 20mer, a second AO was prepared, evaluated, and also found to be ineffective at inducing detectable exon 16 skipping.

Oligonucleotide folding was again analyzed using Mfold,²⁹ and there was no apparent correlation between potential secondary structures and the ability of a compound to induce

exon skipping. For example, H16A(−12 + 19), which induced optimal exon 16 removal, had the potential to self-anneal and form a six A:U duplex, whereas the shorter, inactive

H16A(−07 + 13) could only form a four base A:U duplex (data not shown). This four base A:U duplex was also found in the 25mer H16A(−06 + 19) that induced substantial exon skipping. It is possible that the length and low G:C content of H16A(−07 + 13) may have contributed to the inability to anneal to the target with sufficient affinity to prevent assembly of splicing factors.

The dystrophin pre-mRNA of exon 16, along with flanking intronic sequence, was also analyzed by Mfold. In several predicted structures, there were putative loop-outs that were targeted by the two 31mers, the 25mer H16A(−06 + 19) and the 20mer H16A(−07 + 13). The 20mer annealed precisely to both putative loop-outs, whereas the longer AOs annealed to flanking sequences that were predicted to assume a duplex conformation (data not shown). Again, there was no obvious correlation between binding of the AOs to single-stranded RNA and the ability to induce exon 16 skipping. Limitations of Mfold prediction include analysis of a static segment of sequence, the length of which is somewhat arbitrarily inserted into the program, rather than a nascent gene transcript extruded from the carboxy terminal domain of RNA Pol II, where a complex of proteins and ribonuclear particles assemble on the emerging pre-mRNA.^{31,32}

In the example of exon 16 skipping, we clearly demonstrated that the longer AOs were more efficient at inducing exon

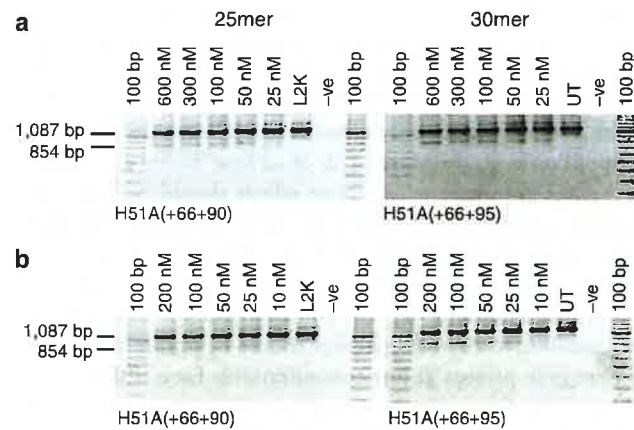


Figure 3 RT-PCR analysis of total RNA from transfected human cells showing exon skipping induced by AOs H51(+66+90) and H51(+66+95) directed at human dystrophin exon 51. The full-length product is 1,087 bp, whereas the product excluding exon 51 is 854 bp. **(a)** Transfection at concentrations ranging from 600 to 25 nM. **(b)** Transfection at concentrations ranging from 200 to 10 nM. Untreated, transfection reagent, and PCR-negative controls are indicated as UT, L2K, and -ve.

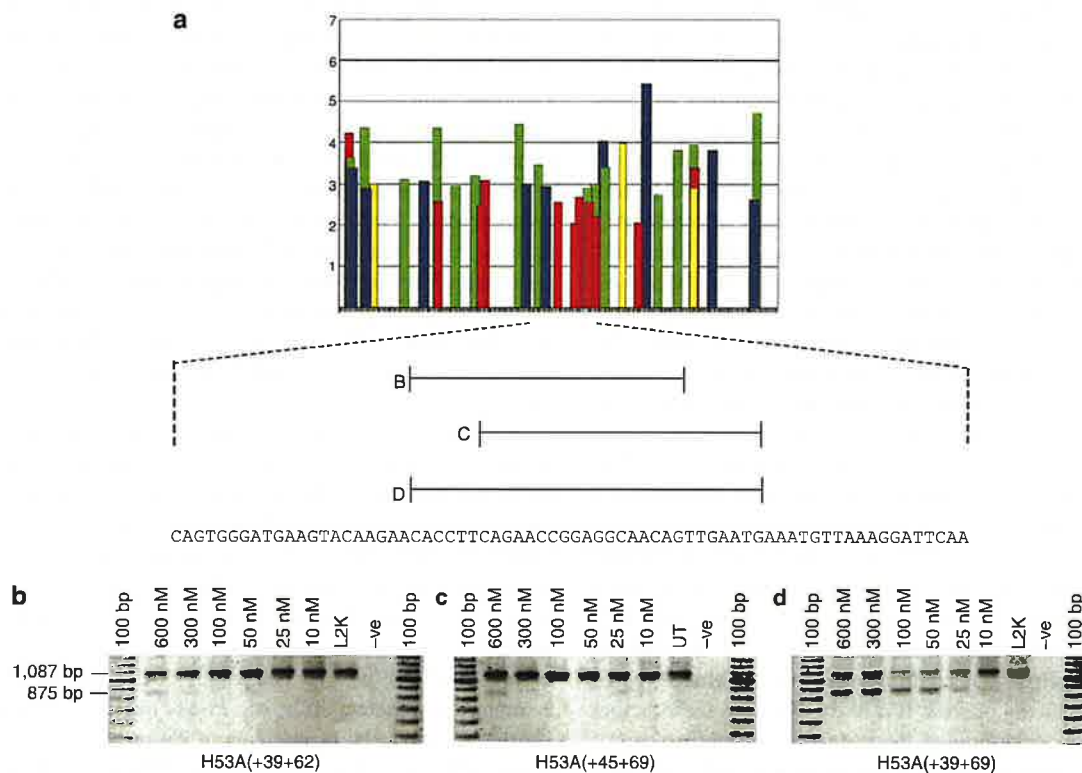


Figure 4 Induction of exon 53 skipping in the human dystrophin gene transcript. **(a)** SR-binding sites for human dystrophin exon 53 as predicted by ESEfinder 2.0, SF2/ASF (red), SC35 (blue), SRp40 (green), and SRp55 (yellow).³⁰ The nucleotide sequence analyzed included the exon 53 sequence and 50 flanking intronic bases. An expanded view shows annealing sites of AOs. **(b-d)** RT-PCR analysis of exon skipping induced by these AOs. The full-length transcript is 1,087 bp, whereas the transcript with exon 53 missing is 875 bp. Untreated, transfection reagent, and PCR controls are indicated as UT, L2K, and -ve.

skipping than overlapping shorter counterparts. These results suggest that the most effective compounds to take to the clinic would be either of the 31mers. In the case of targeting exon 51, this trend was still evident in that some of the longer AOs of 25–30 nucleotides induced higher levels of exon skipping than shorter compounds. However, in this particular example, there was no major difference in efficacy between the overlapping 25 and 30mers. Neither of these AOs targeted any obvious motif predicted to influence splicing, and it is possible that, as yet unidentified factors or secondary structures important in the splicing process were disrupted by the AO annealing. When targeting exon 51, other factors including the ease and cost of AO production may become more significant in the final selection of the optimal compound.

Ease and cost of AO production are not relevant when selecting the preferred compound for exon 53-induced skipping. Overlapping 25mers were only able to induce very low levels of exon 53 skipping, whereas the 31mer induced consistent exon skipping at transfection concentrations as low as 10 nM. Mfold predictions of AO folding indicated that the 31mer H53A(+39+69) could form the same imperfect six base duplex found in H53A(+39+62). The shorter compound has a higher G:C content of 58%, compared to 52% of the 31mer, so it would appear that the strength of annealing is unlikely to be an issue in this example.

There are a number of factors that will influence and effect AO efficacy, including nucleotide sequence. Studies by Matveeva *et al.*³³ have shown certain sequence motifs are associated with poor antisense activity in gene transcript downregulation. It was of interest that these data are not consistent with that for AOs effective at inducing exon skipping. The motif AAAA, which is associated with poor antisense activity for downregulation of gene transcripts, occurs twice in the very effective AO for exon 16, H16A(–12+19) (Table 1). Other factors affecting AO activity include length and chemistry of the modified bases and the nature of the backbone. The modified bases and backbone will greatly impact on the stability of the AO within the cell, and will be crucial to its sustained activity. AOs with the phosphorothioate backbone and 2'-O-methyl modified sugars are subject to degradation by nucleases, but at greatly reduced rates.^{34,35} It has been reported that most AO degradation arises primarily from 3' to 5' exonucleases, and we have shown that modified linkages at the 3' AO terminus can increase and extend exon skipping induction, presumably through increased AO stability.³⁶ It is possible that AOs of greater length may persist longer in the nucleus, thereby conferring activity for an extended period, relative to shorter compounds. As it is presumed that AOs exert their influence by steric hindrance of the splicing machinery, the longer AOs could more effectively block regions essential to the splicing process. It is likely that both these factors influence AO efficiency *in vivo*. Regardless of the mechanism(s), the longer AOs tend to induce more sustained and prolonged exon skipping, but on an exon-by-exon basis, and to date, this has been determined empirically.

It has been proposed that the use of longer AOs may reduce specificity and could induce undesirable exclusion of exons other

than the target.³⁷ Although this possibility cannot be discounted, the conjecture is somewhat pointless if sub-optimal, shorter AOs have to be used at much higher concentrations to induce targeted exon removal. With respect to exon 16, we would estimate the optimal 31mer to be several fold more effective than the best 25mers, based on titration studies where similar levels of exon skipping were induced at 10–25 nM with H16A(–12+19) and between 50 and 100 nM with H16A(–06+19). If the optimal AO can induce substantial levels of exon 16 skipping after application at 10 nM, the risk of adverse events associated with the AO chemistry or off-target effects should be reduced. Annealing to homologous sequences cannot be discounted and we previously demonstrated that an AO with up to five mismatched bases could induce low levels of exon 19 skipping, but only when applied at high concentrations.²⁴ The risk of cross-annealing to related sequences should be minimized if the AOs were only present at low concentrations. Even if there was some crossreaction with homologous sequences, one would anticipate that unless that region contained a splice site, or was involved in initiation of translation, no effects on gene expression would be observed. We have shown in this report that subtle changes in the annealing site of the intended target can play a major role in the efficacy of that compound to modify pre-mRNA processing. The possibility of inadvertently masking another amenable site in a homologous transcript, and altering processing and expression of that RNA strand, must be regarded as remote.

Simply designing an AO of 30 nucleotides will not guarantee induction of exon skipping, and in some cases may be counter-productive, as found when targeting the murine dystrophin exon 23 donor splice site. Our AO designing strategy now involves evaluating AOs of 25 bases, designed to acceptor, donor, and putative ESE motifs, in the primary screen, involving several different *in vitro* transfection concentrations. Subsequent compounds of 25–30 nucleotides are then designed and prepared to those motifs identified in the splicing of the target exon. In the four examples described in this report, amenable sites to redirect dystrophin splicing were identified at the acceptor (human exon 16), 66–95 bases within the 233 base exon 51, 39–69 bases within the 212 base long exon 53, and at the donor splice site of murine exon 23.

In summary, *in silico* predictions may aid in the initial design of AOs to induce targeted exon skipping. There was a trend for the more efficient AOs to target multiple SF2/ASF, SRp40 and SC35 SR motifs, although this was not absolute (Table 2). We suggest that refinement of AO design and identification of amenable sites should be carried out empirically, rather than relying on *in silico* predictions of RNA secondary structure, the masking of obvious splice sites, or predicted ESE motifs. The length of the AO has emerged as a major parameter, AOs of 25–31 nucleotides outperform shorter compounds. In one case, a 25mer was found to be far more effective than overlapping 30mers and a 20mer. In situations where there is no major difference in efficacy between a 25mer and a 31mer, other considerations such as cost and ease of AO production would then become more relevant.

MATERIALS AND METHODS

AO design and synthesis. AOs were synthesized on an Expedite 8909 Nucleic acid synthesizer using the 1 μmol thioate synthesis protocol. Phosphoramidites for synthesis of 2'-O-methyl AOs were purchased from Glen Research (Sterling, VA). Columns were prepared using a DNA synthesis column kit (Applied Biosystems, Melbourne, Australia) with 2'-O-methyl CPG supports from Glen Research. AOs were cleaved overnight at room temperature with ammonium hydroxide (Sigma, Melbourne, Australia) and were desalted on NAP-10 columns (Amersham, Melbourne, Australia). Gram quantities of MD23(-07+18) were obtained from Avecia (Grangemouth, UK).

AOs were synthesized to anneal to splicing motifs at the intron:exon boundaries, as well as ESE motifs predicted by the web-based application, ESEfinder, http://www.ncbi.nlm.nih.gov/entrez/query.fcgi?cmd=Retrieve&db=PubMed&dopt=Citation&list_uids=12824367.³⁰ Table 1 lists the AOs evaluated, the nomenclature indicates target species and annealing coordinates.

Culture and transfection—H-2K^b-tsA58 (H2K) mdx myoblasts. H2K-Mdx myoblasts³⁸ were cultured as described by Mann *et al.*¹⁷ AOs were transfected with Lipofectin:AO at 2:1 w:w ratio, 48 h after seeding. Lipofectin was used according to the manufacturer's instructions (Invitrogen, Melbourne, Australia). All transfections were duplicated and repeated three times to ensure results were reproducible.

Culture and transfection—primary human myoblasts. Primary human myoblasts were prepared from patient biopsies³⁹ supplied by the Department of Neuropathology, Royal Perth Hospital after informed consent. The patient muscle samples were minced with scissors in a few drops of phosphate-buffered saline. The cell slurry was then placed in 2 ml/g (tissue) DMEM (Gibco-Invitrogen, Melbourne, Australia) with 2.4 U/ml of dispase, collagenase, 1% (w/v) (Roche Molecular Biochemicals, Melbourne, Australia), CaCl₂ at 2.4 mM, and the suspension was maintained at 37°C for 30–45 min with occasional mixing by pipette. The cell suspension was then centrifuged at 350 g to sediment the cells. The cells were washed in DMEM and re-suspended in growth medium, Hams F10 with 20% fetal calf serum, 0.5% chick embryo extract (Jomar Diagnostics, Steptey, South Australia), with basic fibroblast growth factor (human, recombinant) (Invitrogen), 10 U/ml penicillin (Invitrogen), 10 μg/ml streptomycin (Invitrogen), and 250 ng/ml amphotericin B (Sigma, Melbourne, Australia), and were cultured at 37°C with 5% CO₂. Re-suspended cells were pre-plated onto uncoated plates to remove fibroblasts; myoblasts were plated onto 100 μg/ml Matrigel- (Australian Biosearch, Perth, Australia) coated flasks and incubated at 37°C with 5% CO₂. The growth media was changed after 3 days. Cells are frozen or sub-cultured when ~70% confluent.

For transfection experiments, tissue culture plates (24 wells) were pre-treated with 50 μg/ml poly D-lysine and 100 μg/ml Matrigel (Australian Biosearch, Perth, Australia). After proliferation, the myoblasts were treated with trypsin and seeded at 2.5 × 10⁴ cells/well in a 24-well plate with DMEM and 5% horse serum (Invitrogen), to encourage differentiation. Primary human myotubes were transfected in Opti-MEM (Invitrogen), 48 h after seeding, with Lipofectamine 2000 (L2K):AO at 1:1 w:w ratio according to the manufacturer's instructions (Invitrogen). For each experiment, transfections were repeated three times to ensure reproducibility of results.

RNA extraction and RT-PCR. RNA was extracted 1, 3, 5, or 7 days after transfection as indicated, using Trizol according to the manufacturer's instructions (Invitrogen). Primer sets for reverse transcription-PCR (RT-PCR) analysis of AO-induced exon skipping were chosen to amplify fragments of the dystrophin gene transcript with several exons flanking

the target exon. This should minimize preferential amplification of smaller products and also allow examination of any effects on flanking exons. RT-PCR was performed on 100 ng total cellular RNA using Titan One-Tube RT-PCR system (Roche Molecular Biochemicals). cDNA was synthesized for 30 min at 48°C, followed by 30 cycles of amplification with cycling conditions of 94°C for 30 s, 55°C for 1 min, and extension at 72°C for 2 min. Primer sequences used for amplification of the mouse transcript are described by Mann *et al.*¹⁷ The primary amplification of exon 16 used primers that anneal to exon 9 forward (cgattcaagagc tatgctac) and exon 18 reverse (gcgagtaacagctgtgaag). Secondary amplification was carried out with primers, 12 forward (taatggatccca gaatcag) and 17 reverse (ccgtagtactgtttccatta). Primary amplification of exons 51 and 53 was performed with exon 47 forward primer (gctccataagcccagaagagc) and exon 58 reverse primer (ctctggtagatgttctc tag). Secondary amplification was carried out with exon 47 forward (tgtgtgtatctctattagg) and exon 58 reverse primers (ctctggtagatgttctc tag). One microliter of the RT-PCR product was used as the target for secondary amplification following 6-min incubation at 94°C and 30 cycles using AmpliTaq-Gold (Applied Biosystems, Melbourne, Australia). PCR products were fractionated on 2% Tris-acetate EDTA buffer agarose gel and stained with ethidium bromide. Images were recorded with a Chemi-Smart 3000 gel documentation system (Vilber Lourmat, Marne La Vallee).

Sequencing. The RT-PCR products were re-amplified by bandstab⁴⁰ and purified using Ultraclean PCR clean up DNA purification kit from Mo-bio (Geneworks, Adelaide, Australia). The purified products were sequenced using an Applied Biosystems 377 DNA sequencer and BigDye V3.1 terminator chemistry (Applied Biosystems). Sequencing PCR conditions were 25 cycles of 96°C for 30 s, 50°C for 30 s, and 60°C for 4 min.

ACKNOWLEDGMENTS

The authors received funding from aktion benni and co e.V., Germany, the National Institutes of Health (RO1NS044146-02), the Muscular Dystrophy Association USA (MDA3718), the National Health and Medical Research Council of Australia (303216), and the Medical and Health Research Infrastructure Fund (Western Australia). The technical assistance of B Gebiski is acknowledged.

REFERENCES

1. Monaco, AP (1989). Dystrophin, the protein product of the Duchenne/Becker muscular dystrophy gene. *Trends Biochem Sci* **14**: 412–415.
2. Leon, SH, Schuffler, MD, Kettler, M and Rohrmann, CA (1986). Chronic intestinal pseudoobstruction as a complication of Duchenne's muscular dystrophy. *Gastroenterology* **90**: 455–459.
3. Emery, AE (1989). Clinical and molecular studies in Duchenne muscular dystrophy. *Prog Clin Biol Res* **306**: 15–28.
4. Muntoni, F, Torelli, S and Ferlini, A (2003). Dystrophin and mutations: one gene, several proteins, multiple phenotypes. *Lancet Neurol* **2**: 731–740.
5. Roberts, RG, Coffey, AJ, Bobrow, M and Bentley, DR (1993). Exon structure of the human dystrophin gene. *Genomics* **16**: 536–538.
6. Den Dunnen, JT *et al.* (1989). Topography of the Duchenne muscular dystrophy (DMD) gene: FIGE and cDNA analysis of 194 cases reveals 115 deletions and 13 duplications. *Am J Hum Genet* **45**: 835–847.
7. Monaco, AP, Bertelson, CJ, Liechti-Gallati, S, Moser, H and Kunkel, LM (1988). An explanation for the phenotypic differences between patients bearing partial deletions of the DMD locus. *Genomics* **2**: 90–95.
8. England, SB *et al.* (1990). Very mild muscular dystrophy associated with the deletion of 46% of dystrophin. *Nature* **343**: 180–182.
9. Heald, A, Anderson, LV, Bushby, KM and Shaw, PJ (1994). Becker muscular dystrophy with onset after 60 years. *Neurology* **44**: 2388–2390.
10. Beggs, AH *et al.* (1991). Exploring the molecular basis for variability among patients with Becker muscular dystrophy: dystrophin gene and protein studies. *Am J Hum Genet* **49**: 54–67.
11. Dominski, Z and Kole, R (1993). Restoration of correct splicing in thalassemic pre-mRNA by antisense oligonucleotides. *Proc Natl Acad Sci USA* **90**: 8673–8677.
12. Wilton, SD *et al.* (1999). Specific removal of the nonsense mutation from the mdx dystrophin mRNA using antisense oligonucleotides. *Neuromuscul Disord* **9**: 330–338.
13. van Deutekom, JC and van Ommen, GJ (2003). Advances in Duchenne muscular dystrophy gene therapy. *Nat Rev Genet* **4**: 774–783.

14. Bulfield, G, Siller, WG, Wight, PA and Moore, KJ (1984). X chromosome-linked muscular dystrophy (mdx) in the mouse. *Proc Natl Acad Sci USA* **81**: 1189–1192.
15. Sicinski, P, Geng, Y, Ryder-Cook, AS, Barnard, EA, Darlison, MG and Barnard, PJ (1989). The molecular basis of muscular dystrophy in the mdx mouse: a point mutation. *Science* **244**: 1578–1580.
16. Duncley, MG, Manoharan, M, Villiet, P, Eperon, IC and Dickson, G (1998). Modification of splicing in the dystrophin gene in cultured Mdx muscle cells by antisense oligonucleotides. *Hum Mol Genet* **7**: 1083–1090.
17. Mann, CJ *et al.* (2001). Antisense-induced exon skipping and synthesis of dystrophin in the mdx mouse. *Proc Natl Acad Sci USA* **98**: 42–47.
18. Muntoni, F, Bushby, K and van Ommen, G (2005). 128th ENMC International Workshop on 'Preclinical optimization and Phase I/II Clinical Trials Using Antisense Oligonucleotides in Duchenne Muscular Dystrophy' 22–24 October 2004, Naarden, The Netherlands. *Neuromuscul Disord* **15**: 450–457.
19. Aartsma-Rus, A *et al.* (2004). Antisense-induced multiexon skipping for Duchenne muscular dystrophy makes more sense. *Am J Hum Genet* **74**: 83–92.
20. Agrawal, S (1999). Importance of nucleotide sequence and chemical modifications of antisense oligonucleotides. *Biochim Biophys Acta* **1489**: 53–68.
21. Lebedeva, I and Stein, CA (2001). Antisense oligonucleotides: promise and reality. *Annu Rev Pharmacol Toxicol* **41**: 403–419.
22. Bremmer-Bout, M *et al.* (2004). Targeted exon skipping in transgenic hDMD mice: a model for direct preclinical screening of human-specific antisense oligonucleotides. *Mol Ther* **10**: 232–240.
23. Chelly, J, Montarras, D, Pinset, C, Berwald-Netter, Y, Kaplan, JC and Kahn, A (1990). Quantitative estimation of minor mRNAs by cDNA–polymerase chain reaction. Application to dystrophin mRNA in cultured myogenic and brain cells. *Eur J Biochem* **187**: 691–698.
24. Errington, SJ, Mann, CJ, Fletcher, S and Wilton, SD (2003). Target selection for antisense oligonucleotide induced exon skipping in the dystrophin gene. *J Gene Med* **5**: 518–527.
25. Takeshima, Y *et al.* (2001). Oligonucleotides against a splicing enhancer sequence led to dystrophin production in muscle cells from a Duchenne muscular dystrophy patient. *Brain Dev* **23**: 788–790.
26. Pramono, ZA, Takeshima, Y, Alimsardjono, H, Ishii, A, Takeda, S and Matsuo, M (1996). Induction of exon skipping of the dystrophin transcript in lymphoblastoid cells by transfecting an antisense oligodeoxynucleotide complementary to an exon recognition sequence. *Biochem Biophys Res Commun* **226**: 445–449.
27. Mann, CJ, Honeyman, K, McClorey, G, Fletcher, S and Wilton, SD (2002). Improved antisense oligonucleotide induced exon skipping in the mdx mouse model of muscular dystrophy. *J Gene Med* **4**: 644–654.
28. Lu, IL *et al.* (2003). Correction/mutation of acid alpha-D-glucosidase gene by modified single-stranded oligonucleotides: *in vitro* and *in vivo* studies. *Gene Therapy* **10**: 1910–1916.
29. Zuker, M (2003). Mfold web server for nucleic acid folding and hybridization prediction. *Nucleic Acids Res* **31**: 3406–3415.
30. Cartegni, L, Wang, J, Zhu, Z, Zhang, MQ and Krainer, AR (2003). ESEfinder: a web resource to identify exonic splicing enhancers. *Nucleic Acids Res* **31**: 3568–3571.
31. Maniatis, T and Reed, R (2002). An extensive network of coupling among gene expression machines. *Nature* **416**: 499–506.
32. Reed, R (2003). Coupling transcription, splicing and mRNA export. *Curr Opin Cell Biol* **15**: 326–331.
33. Matveeva, OV *et al.* (2000). Identification of sequence motifs in oligonucleotides whose presence is correlated with antisense activity. *Nucleic Acids Res* **28**: 2862–2865.
34. Crooke, RM, Graham, MJ, Cooke, ME and Crooke, ST (1995). *In vitro* pharmacokinetics of phosphorothioate antisense oligonucleotides. *J Pharmacol Exp Ther* **275**: 462–473.
35. Agrawal, S, Temsamani, J and Tang, JY (1991). Pharmacokinetics, biodistribution, and stability of oligodeoxynucleotide phosphorothioates in mice. *Proc Natl Acad Sci USA* **88**: 7595–7599.
36. GebSKI, BL, Errington, SJ, Johnsen, RD, Fletcher, S and Wilton, SD (2005). Terminal antisense oligonucleotide modifications can enhance induced exon skipping. *Neuromuscul Disord* **15**: 622–629.
37. Graham, IR, Hill, VJ, Manoharan, M, Inamati, GB and Dickson, G (2004). Towards a therapeutic inhibition of dystrophin exon 23 splicing in mdx mouse muscle induced by antisense oligonucleotides (splicomers): target sequence optimisation using oligonucleotide arrays. *J Gene Med* **6**: 1149–1158.
38. Morgan, JE *et al.* (1994). Myogenic cell lines derived from transgenic mice carrying a thermolabile T antigen: a model system for the derivation of tissue-specific and mutation-specific cell lines. *Dev Biol* **162**: 486–498.
39. Rando, TA and Blau, HM (1994). Primary mouse myoblast purification, characterization, and transplantation for cell-mediated gene therapy. *J Cell Biol* **125**: 1275–1287.
40. Wilton, SD, Lim, L, Dye, D and Laing, N (1997). Bandstab: a PCR-based alternative to cloning PCR products. *Biotechniques* **22**: 642–645.